F layer postsunset height rise due to electric field prereversal enhancement: 2. Traveling planetary wave ionospheric disturbances and their role on the generation of equatorial spread *F*

P. R. Fagundes,[1] J. R. Abalde,[1] J. A. Bittencourt,[2] Y. Sahai,[1] R. G. Francisco,[1] V. G. Pillat,[1] and W. L. C. Lima[3]

Received 25 May 2009; revised 27 July 2009; accepted 21 August 2009; published 30 December 2009.

[1] This paper investigates the role played by traveling planetary wave ionospheric disturbances (TPWIDs) on the modulation of the electric field prereversal enhancement (PRE) amplitude, near-sunset hours, in the equatorial ionosphere, and their influence on the day-to-day equatorial spread *F* (ESF) variability. We show that ''fresh'' (ESF) day-to-day variability is closely related with the postsunset height rise due to the electric field PRE, and there is some indication that the altitude of 300 km may be a threshold height for the generation of fresh ESF. Observations of *F* layer virtual heights during evening hours (1800 LT, 1900 LT, and 2000 LT) present a strong day-to-day variability, even during geomagnetically quiet periods. In fact, this well-organized variability is induced by TPWIDs-type oscillations that push the *F* layer up or down according to the TPWID phase. The preliminary analysis presented here show that, when the planetary TPWID oscillations or geomagnetic activity raises the *F* layer around sunset hours, the occurrence of fresh ESF is increased, but when the TPWID-type oscillations or geomagnetic activity pushes the *F* layer downward, the fresh ESF occurrence is reduced. Also, the TPWID phase modulated the onset time of the fresh ESF during high fresh ESF season. The modulation acts in such way that, when the TPWID phase maximizes, the fresh ESF onset time occurs earlier than when the TPWID phase minimizes and the fresh ESF onset time occurs later.

Citation: Fagundes, P. R., J. R. Abalde, J. A. Bittencourt, Y. Sahai, R. G. Francisco, V. G. Pillat, and W. L. C. Lima (2009), *F* layer postsunset height rise due to electric field prereversal enhancement: 2. Traveling planetary wave ionospheric disturbances and their role on the generation of equatorial spread *F*, *J. Geophys. Res.*, *114*, A12322, doi:10.1029/2009JA014482.

1. Introduction

[2] Equatorial spread *F* (ESF) has been studied since late 1930s [*Booker and Wells*, 1938]. Nevertheless, it continues to attract considerable attention nowadays as debate is going on regarding the onset conditions and the possible causes for the day-to-day ESF variability. Multiinstruments observations from both ground (optical, ionosondes, and radars) and space (rockets and satellites) have been applied since late 1930s to understand ESF, but still there are several open questions regarding the day-to-day ESF variability. However, our knowledge about ESF seasonal and solar cycle variation, morphology (zonal and meridional dimension), zonal drift speed has improved considerably [*Abalde et al.*, 2001, 2004, 2009; *Abdu*, 2001; *Abdu et al.*, 1992; *Bittencourt et al.*, 1997; *Fritts et al.*, 2008; *Kil et al.*, 2004; *Mendillo et al.*, 1992, 2001, 2005; *Pimenta et al.*, 2001a, 2001b, 2003; *Rao et al.*, 1997; *Sahai et al.*, 2000; *Sobral et al.*, 2002; *Sreeja et al.*, 2009; *Sultan*, 1996; *Terra et al.*, 2004; *Tsunoda*, 2005, 2009; *Woodman*, 2009].

[3] It is well accepted that the fundamental mechanism of ionospheric large- and medium-scale irregularities is the Rayleigh-Taylor instability (R-T) [*Saito and Maruyama*, 2006; *Sultan*, 1996]. However, to initiate the R-T instability a precursor is needed, acting on the F layer bottom side, to generate a small perturbation on the electron density. Gravity waves (GWs) have been proposed, for a long time, as the best candidate for this purpose [*Ossakow*, 1981; *Sastri et al.*, 1997; *Sekar et al.*, 1995]. In spite of the fact that GWs appear to be the best candidate to trigger the R-T instability, all the experiment and observation campaigns carried out to confirm such dependence have not found a one-to-one relationship between GW and ESF generation. As pointed out by *Klausner et al.* [2009] GWs and traveling ionospheric disturbances (TIDs) at low-latitude *F* layer are present at low-latitude *F* layer almost every day with different amplitudes and wavelengths. However, ESF clearly presented seasonal variation with maximum from September to March and minimum during June to August, in the American sector. This seems to be a good indication that GW alone does not explain the day-to-day ESF variability.

[1] Universidade do Vale do Paraíba, Sao Jose dos Campos, Brazil.
[2] Instituto Nacional de Pesquisas Espaciais, Sao Jose dos Campos, Brazil.
[3] Centro Universitário Luterano de Palmas, Palmas, Brazil.

0148-0227/09/2009JA014482

[4] The day-to-day variability of the thermosphere and ionosphere, during geomagnetic quiet periods, has also been related to planetary waves (PWs), gravity waves (GWs) and thermospheric winds [*Abdu et al.*, 2006a, 2006b, 2006c; *Fagundes et al.*, 1995, 1999, 2007; *Devasia et al.*, 2002; *Jyoti et al.*, 2004; *Klausner et al.*, 2009; *Nicolls and Kelley*, 2005; *Pancheva et al.*, 2006; *Takahashi et al.*, 2005, 2006, 2007; *Vineeth et al.*, 2007]. It is well known that GWs are generated locally and have periods from minutes to hours. However, PW oscillations have global scales with periods ranging from 2 to 30 days. According to *Lastovicka et al.* [2003], sources for this kind of waves are predominantly tropospheric or of geomagnetic activity. Also, *Fagundes et al.* [2005] showed that waves with longer periods of about 27 days and 13.5 days are related to solar and half solar rotation, respectively.

[5] In this investigation, traveling planetary wave ionospheric disturbances (TPWIDs) are used to refer to oscillations of a given ionospheric parameter (virtual height), with periods of days [*Fagundes et al.*, 2009]. This terminology is used in analogy to traveling ionospheric disturbances (TIDs) associated to GW oscillations in the neutral atmosphere.

[6] In this paper we present and discuss observations of day-to-day ESF variations associated with *F* layer virtual height variations during evening hours (1800 LT to 2000 LT), carried out at Palmas (10.2°S, 48.2°W, dip latitude 5.5°S, hereafter PAL), Brazil. This study shows that TPWIDs, with periods of several days, control the strength of the electric field PRE and, therefore, slowly push the *F* layer height up and down, according to the TPWID phase. The postsunset *F* layer vertical drift, induced by TPWIDs, acts to create favorable or unfavorable conditions to generate ESF.

2. Data Analysis and Discussion

[7] In this study we have analyzed ionospheric sounding data obtained at PAL, by an ionosonde-type CADI. The ionosonde operates simultaneously in two different modes. The first mode scan 180 frequencies every 300 s (normal ionogram with temporal resolution of 300 s) and the second mode scan only 6 fixed frequencies (3, 4, 5, 6, 7, and 8 MHz) every 100 s (ionograms with lower spectral resolution, but with high temporal resolution of 100 s). For more details see *Fagundes et al.* [2005, 2007, 2009] and *Klausner et al.* [2009].

[8] Figures 1a and 1b show examples of ionogram echoes from the *E* and *F* layers for two different days, with and without spread *F*. These ionograms were obtained using the second mode of operation for 1800 LT, 1900 LT, 2000 LT, and 2100 LT, during the occurrence of the electric field PRE. Figure 1a shows echoes obtained on 4 August 2003 (low ESF season), and illustrates the dynamics of the *F* layer during the electric field PRE when there is no occurrence of ESF. Notice that at 1800 LT the virtual height of the *F* layer at 3 MHz is around 250 km and, during the other three chosen times, there was no uplifting of the *F* layer, but the virtual height at 7 MHz presented a small uplift between 2300 LT and 2400 LT. Consequently, under this condition of ionospheric dynamics, no ESF was generated. On the other hand, on 22 December 2003 (Figure 1b, high ESF season) the dynamics of the *F* layer is completely different. At 1800 LT the virtual height is around 270 km at 3 MHz and a strong uplift takes place up to 2000 LT, when the virtual height reaches around 400 km. Then, at 2100 LT, it is clearly seen the multiple echoes at 3, 4, and 7 MHz, which is the signature of ESF on the ionogram. The uplifting of the *F* layer during the electric field PRE has been suggested as one of the key ingredients for the generation of spread *F* [*Lee et al.*, 2005, *Saito and Maruyama*, 2006].

[9] In order to show in more detail the connection between the electric field PRE and ESF occurrence, Figures 2 and 3 are included to illustrate some cases where the vertical ionospheric motions play an important role on ESF generation. Figures 2 and 3 show the daily virtual height variations for six fixed frequencies (3, 4, 5, 6, 7, and 8 MHz) using the data observed every 100 s, as well as the daily *Dst* index variations. The ionospheric data were obtained at PAL on 23–25 October 2003 (Figure 2) and 16–23 August 2003 (Figure 3). It is important to mention that this investigation is concerned mainly with the conditions for generation and the onset time of equatorial ionospheric irregularities, so that only ESFs detected between 1800 LT to 2100 LT (''fresh'' irregularities), generated near the observation site, are considered. ESFs observed later are assumed to represent ''fossil'' equatorial ionospheric irregularities that are generated far away from the site [*Saito and Maruyama*, 2006] and drift to eastward reaching the observation site after 2100 LT.

[10] The three consecutive days on October were selected to illustrate the daily virtual height variations, the day-to-day variation of the electric field PRE and ESF occurrences during high spread *F* season. Notice that on 23–24 and 25–26 October 2003 there is a strong electric field PRE reaching its maximum around 2200 UT (1900 LT) and, just after that, multiechoes are observed in several frequencies, which represent the signature of spread *F*. However, on 24 October 2003 the electric field PRE reach heights lower than those for the previous and subsequent days and, as a consequence, no ESF was formed. Notice that the *Dst* index was a bit disturbed on 24–25 October, indicating that changes on geomagnetic activity can induce significant changes on the behavior of the electric field PRE and, consequently, on the control of the day-to-day ESF occurrence.

[11] During 16–23 August 2003 (Figure 3), which is representative of the low spread *F* season, there are three days in which ESF was not generated (15–16, 16–17, and 22–23 August) and other three days (19–20, 20–21, and 21–22 August) which range spread *F* was generated after 2300 UT (2100 LT). Nevertheless, during 17–18, 18–19, and 19–20 August multiple echoes are seen just after 2300 UT (2000 LT), which are a signature of ESF. A perusal of Figures 2 and 3 shows that when, during all days, the *F* layer bottom side reached higher altitudes during postsunset height rise, as compared to the other days, there is generation of ESF. Again, there is clear evidence that the electric field PRE has a strong influence on the day-to-day ESF variation.

[12] The main purpose of this investigation is to analyze the effects of traveling planetary wave ionospheric disturbance (TPWID)-type oscillations on the *F* layer postsunset height rise and their role on the generation of equatorial spread *F*. Therefore, the same methodology described by

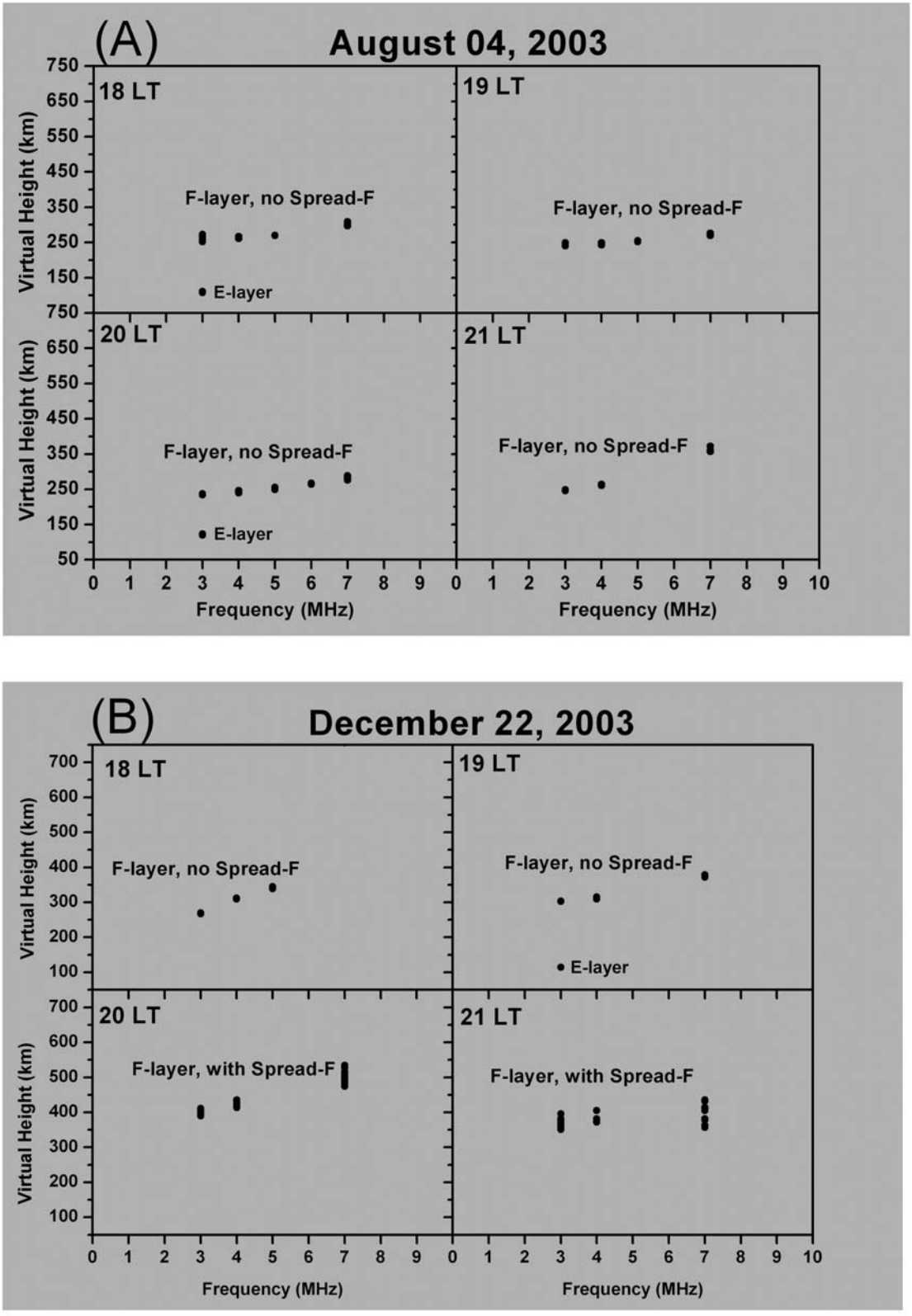

Figure 1. Sets of ionograms obtained with lower spectral resolution at Palmas on 4 August 2003 and 22 December 2003. (a) Echoes during the electric field PRE when there is no occurrence of spread *F*. (b) Echoes during the electric field PRE when there is occurrence of spread *F*.

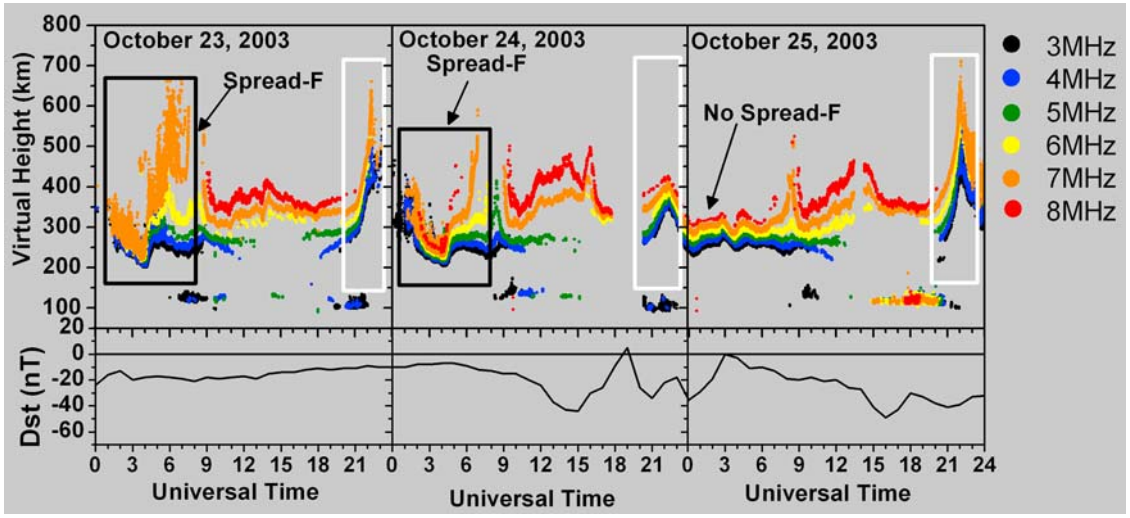

Figure 2. Virtual height variations for 3, 4, 5, 6, 7, and 8 MHz (isofrequency plots) for the period 23–25 October 2003 observed at (top) PAL and (bottom) *Dst* variation. The white and black rectangles indicate the postsunset height rise associated with zonal electric field prereversal enhancement and spread *F* occurrences, respectively.

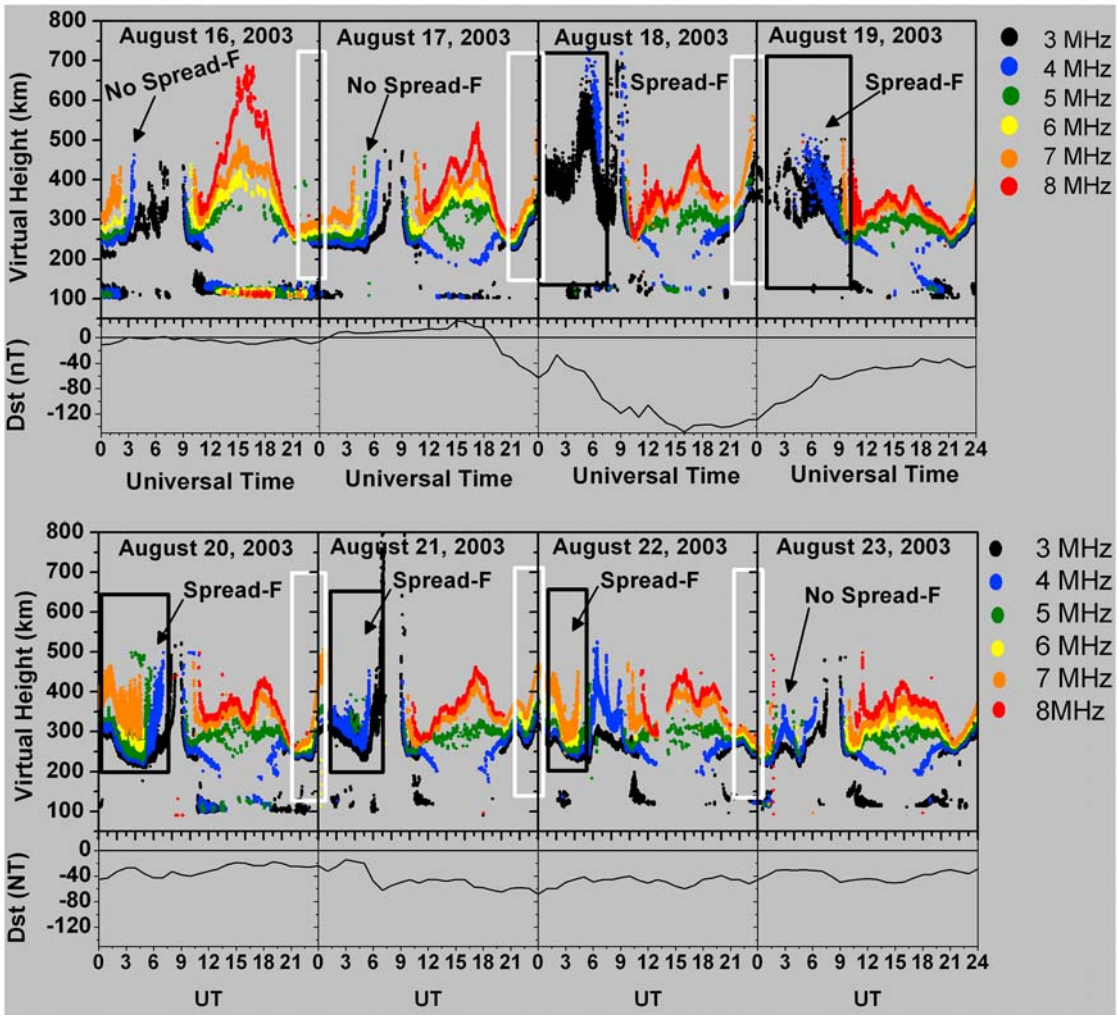

Figure 3. Virtual height variation for 3, 4, 5, 6, 7, and 8 MHz (isofrequency plots) for the period 16–20 August 2003 observed at PAL. The white and black rectangles indicate the postsunset rise associated with the zonal electric field PRE and spread *F* occurrence, respectively.

Fagundes et al. [2005, 2009] to study TPWID at *F* layer heights is used here, but considering the appropriate local times after sunset hours.

[13] The *F* layer virtual height for each day at three fixed local times (1800 LT, 19:00 LT, and 2000 LT) at five selected frequencies (3, 4, 5, 6, and 7 MHz), for the period July 2003 to May 2004, are considered and analyzed in this study. These local times were chosen because the electric field PRE uplift the *F* layer between about 1900 LT and 2000 LT, and the strength and duration of the electric field PRE will create favorable or adverse conditions for ESF generation. This technique allows the investigation of the day-to-day evolution of the virtual height variations at some fixed frequencies. In the absence of waves, with periods of days, controlling the movement of the *F* layer, we may expect random virtual height day-to-day variations, but, on the other hand, if the virtual height day-to-day variations show a modulation with periods of days, this is an indication of the presence of TPWID-type oscillations modulating the virtual height. Figures 4 and 5 illustrate that the day-to-day virtual height variations for all frequencies show wave-like oscillations. The modulation caused by TPWID-type oscillations is present during both geomagnetically quiet and disturbed periods.

[14] Figures 4 and 5 (from July to December 2003 from January to May 2004) show three panels for each month. The upper panel gives the day-to-day ESF history for each month, where the red bars indicate the range spread *F* (when the traces away from critical frequency (foF2) show broadening in range or the presence of satellite traces), blue bars indicate the frequency spread *F* (when the traces near critical frequency (foF2) are broadened), white bars indicate no data and dotted lines indicate days with no ESF. The full black line link ESF onset time on consecutive days (This give a roughly idea of the day-to-day variation of the ESF onset time) and the dark gray full rectangles denote the time of occurrence of fresh ESF (1800 LT to 2100 LT). The middle and bottom panels for each month show the day-to-day virtual height variations at 1900 LT and 2000 LT, respectively. The large open squares show the geomagnetic disturbed periods and its respectively minimum *Dst* values and the black horizontal line is a reference line at 300 km.

[15] It is seen that, during the period from July 2003 to May 2004, there are signatures of TPWID-type oscillations controlling the electric field PRE amplitude and, therefore, controlling the speed of vertical plasma drift that will finally determine the *F* layer bottom side height. However, the TPWID-type oscillations, with periods of days, that modulate the virtual height day-to-day variations during the electric field PRE, may be strongly suppressed by geomagnetic storm prompt penetration, or disturbed dynamo, electric fields and, therefore, push up or down the *F* layer according to the zonal electric field polarization (eastward electric field pushes up and westward electric field pushes down). Since the formation of ESF is strong controlled by the *F* layer bottom side height, then the TPWID phase and disturbed electric field play an important role on ESF generation.

[16] The data presented in Figure 4 correspond to July to December 2003 and in Figure 5 correspond to January to May 2004. The first two months (July and August 2003) are typical of low fresh ESF season (see upper panel for July and August) that are characterized by a weak electric field PRE, as compared with the high fresh ESF season (October to March), but, from time to time, stronger electric field PRE can be seen and it is possible to see fresh ESF forming (starting between 1800 LT and 2100 LT). On the other hand the numbers of nights that the ESF appears in the ionosonde field of view after 2100 LT (''fossil'' ESF), or nights without ESF, are frequent during low fresh ESF season.

[17] A perusal on the middle and bottom panels of July and August (Figure 4) and May (Figure 5) clearly shows that the virtual height is oscillating around 300 km and, when the TPWID phase maximizes (see 5 July, 19–20 July, and 1 August) or geomagnetic activity (see 17–18 August) uplifts the *F* layer, there is occurrence of fresh ESF over PAL. This may explain the day-to-day variability of fresh ESF occurrence during low spread *F* season.

[18] By the end of September (Figure 4 – middle panels) a transition occurs from low to high ESF season. Notice that, by the beginning of September, the *F* layer bottom side at 1900 LT and 2000 LT is bellow 300 km of altitude, but later (after 22 September) the *F* layer heights begin to move upward, reaching altitudes above 300 km. During the first half of September (upper panel) it is noticed that there are no ESF occurrences when the TPWID phase minimizes (see 1, 2, 9, 10, and 15 September), but for other nights, when the TPWID phase maximizes, there are fresh ESF generation. After 22 September it is clearly seen that the *F* layer bottom side moves rapidly to heights higher than 300 km and, at the same time, there are oscillations with weak amplitudes and the fresh ESF onset time occurs earlier as the *F* layer bottom side is getting higher and higher in altitude. Also, it is noticed a day-to-day oscillation on the fresh ESF onset time, after 22 September, that has a strong anticorrelation with the day-to-day bottom side *F* layer TPWID wave like oscillations. In such way, when the virtual height is higher, the fresh ESF is generated earlier, and when the virtual height is lower (but higher than 300 km), the fresh ESF is generated later. This indicates that the *F* layer bottom side height not only create favorable or adverse conditions for generation of fresh ESF, but also control the onset time of fresh ESF during high ESF season.

[19] From October to March occurs the high ESF season (Figures 4 and 5), and the influence of TPWID-type oscillations on ESF generation is quite different. Now, almost every day there is occurrence of fresh spread *F* over PAL, the only exception being when the TPWID phase minimizes and lowers the *F* layer, so that there is no ESF formation, or ESF is observed after 2100 LT (''fossil'' ESF), or when the disturbed electric field pushes down the *F* layer (11 and 20 November; 30 and 31 December; 7, 16, 23, and 30 January; 1–4, 6–9, 11, 13–14, 22, 24, and 27 February; and 11, 14, 18–19, 26, and 28 March).

[20] During the high ESF season it is clearly noticed how the TPWID phase controls the onset time of ESF generation. For more details refer to the day-to-day virtual height variation on 1–20 November at 1900 LT. It is possible to see a TPWID with maximum phase around 4–5 November, a minimum phase around 12–13 November and, again, a maximum phase around 19 November. This observation period is very interesting because a monochromatic TPWID, with a period of about 15 days, is propagating in the *F* layer, and the onset time of the fresh ESF takes place

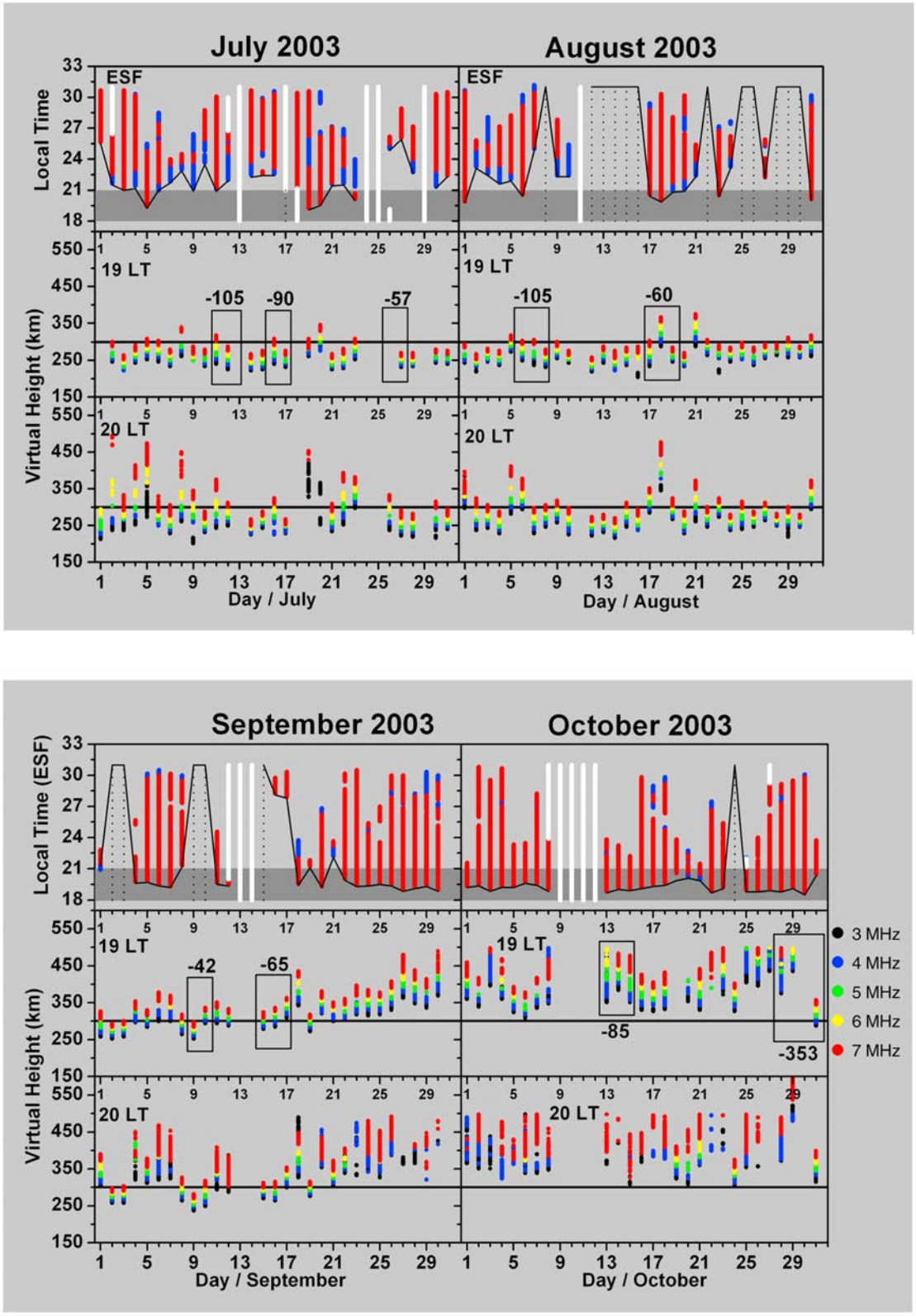

Figure 4. The top panel for each month show day-to-day history of ESF (range and frequency) from July to December 2003, where red is range spread *F*, blue is frequency spread *F*, white is absence of data, and dotted line is night with absence of ESF. The full black line links the ESF onset time, and the dark gray rectangles highlight the time occurrence of fresh ESF. The middle and bottom panels for each month show the daily virtual height variations for the 3, 4, 5, 6, and 7 MHz frequencies selected for (middle panel) 1900 LT and (bottom panel) 2000 LT, respectively, for the period of July to December 2003. Open squares indicate geomagnetic disturbed periods with its minimum *Dst* index, respectively.

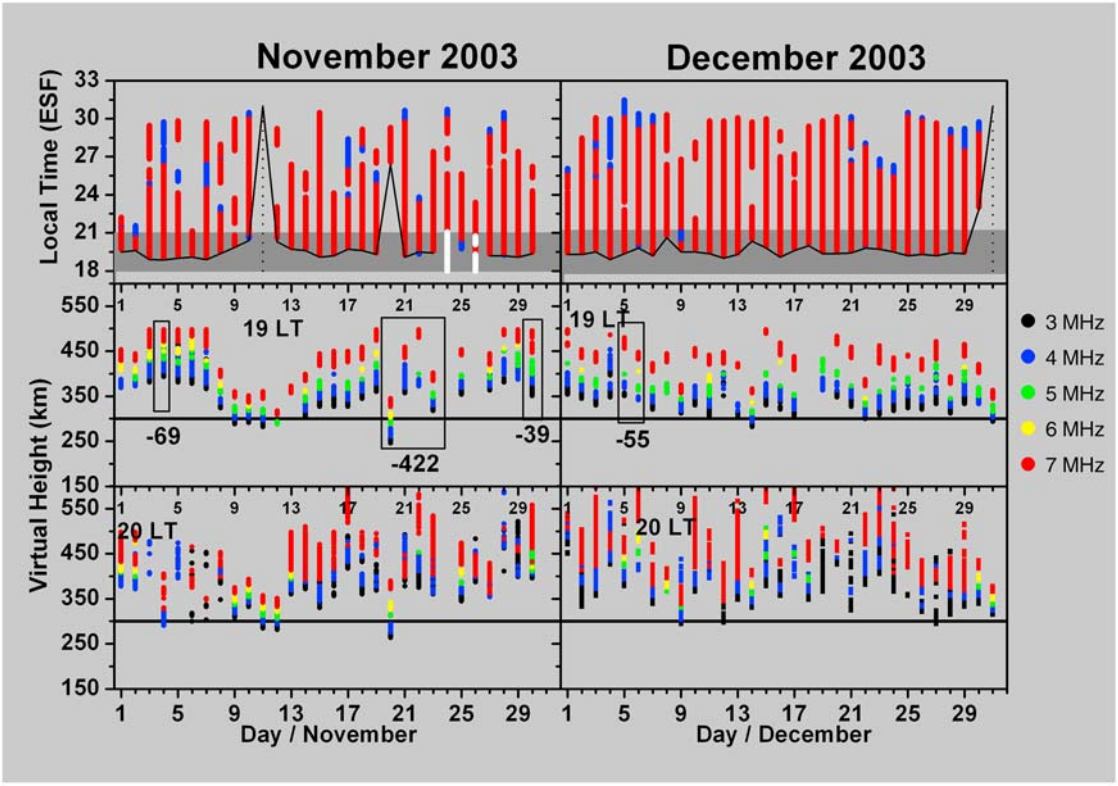

Figure 4. (continued)

early when the TPWID phase maximizes. As the TPWID phase move to minimum, the fresh ESF onset time takes place later and, finally, when the TPWID phase minimizes, there is no ESF formation.

[21] By the end of March and beginning of April (Figure 5), a transition from high to low spread *F* season takes place. During the months from October to March the electric field PRE was strong and the *F* layer virtual heights are above 300 km. However, during the March–April months, the *F* layer virtual heights are below 300 km. During the end of March and April there are only a few cases of fresh ESF occurrence (21–25, 28, and 29–31 March and 1–3, 6, and 19 April) and "fossil" ESF and non-ESF are more frequently cases during April.

[22] The present data clearly shows that TPWID-type oscillations, with periods of days, play a key role in ESF formation, but their role is different during the low and high ESF seasons. During the low ESF season the TPWID-type oscillations contributed to the generation of ESF, when the TPWID maximum phase uplifts the layer above 300 km, thus creating favorable conditions for ESF formation. However, during high ESF season, the TPWID minimum phase pushes down the *F* layer to heights less than 300 km, thus creating conditions unfavorable for ESF generation. In addition, the TPWID phase controls the onset time of ESF, and there is an anticorrelation between the TPWID phase and the onset time ESF generation, i.e., when the *F* layer is oscillating with period of days, but above of 300 km, the ESF onset time takes place earlier during the TPWID maximum phase and later during the TPWID minimum phase.

[23] The day-to-day ESF unpredictability is still a fact, in spite of the theoretical and observational efforts that have been made during several decades (for more details see *Woodman* [2009, and references therein] and *Tsunoda* [2005, 2009]). *Tsunoda* [2005, 2009] proposed that a large-scale wave structure (LSWS) could be associated with the generation of ESF and concluded that LSWS development, together with the zonal drift shear, may contribute to day-to-day ESF variability. On the other hand, *Woodman* [2009] proposed that a horizontal plasma drift counterstreaming with the neutral wind at the steep *F* region bottom side could produces a fast growing instability and, consequently formation of ESF.

[24] The present work shows that the strength of the electric field PRE can uplift the *F* layer to more unstable altitudes or maintain the *F* layer on heights where the generation of fresh ESF is adverse. But, more important, there are traveling planetary wave ionospheric disturbances that modulate the electric field PRE and then control the day-to-day ESF variability and the onset time.

3. Conclusions

[25] Ionospheric *F* layer sounding observations, using a Canadian Advanced Digital Ionosonde (CADI), have been carried out at Palmas (10.2°S, 48.2°W, dip latitude 5.5° S, near-equatorial region), Brazil. The main purpose of this paper is to investigate how traveling planetary wave ionospheric disturbances (TPWID)-type oscillations modulate the electric field PRE, near-sunset hours, in the equatorial ionosphere, and, consequently, how they influence the day-

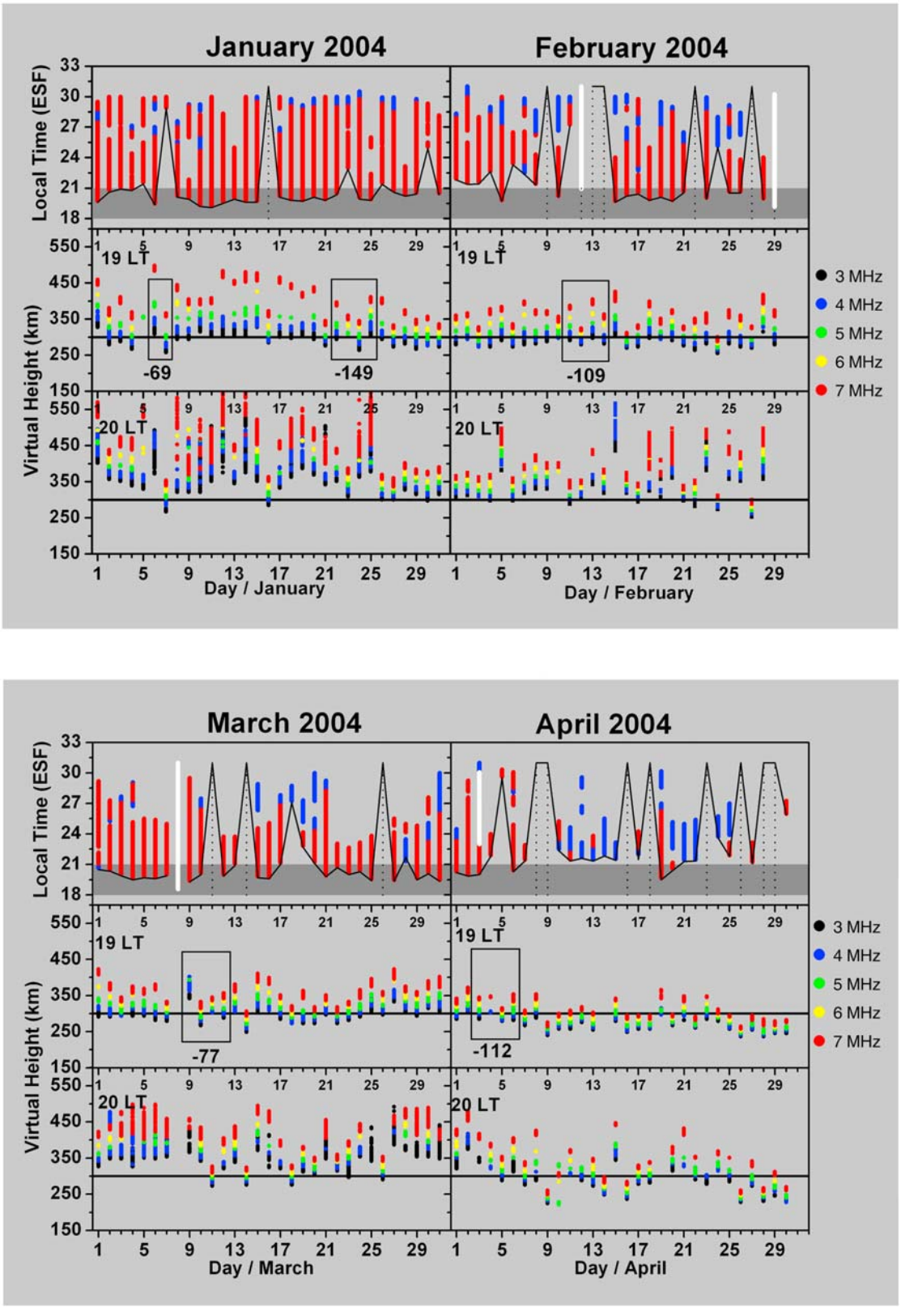

Figure 5. The same in Figure 4 but for January to May 2004.

to-day ESF variability, since the generation of ESF and the vertical plasma drift, due to the electric field PRE, are strongly connected. The main results are summarized below:

[26] 1. The occurrence of fresh ESF at PAL is strongly controlled by the *F* layer height during the electric field PRE. There is some indication that the altitude of 300 km may be a threshold height for the generation of fresh ESF.

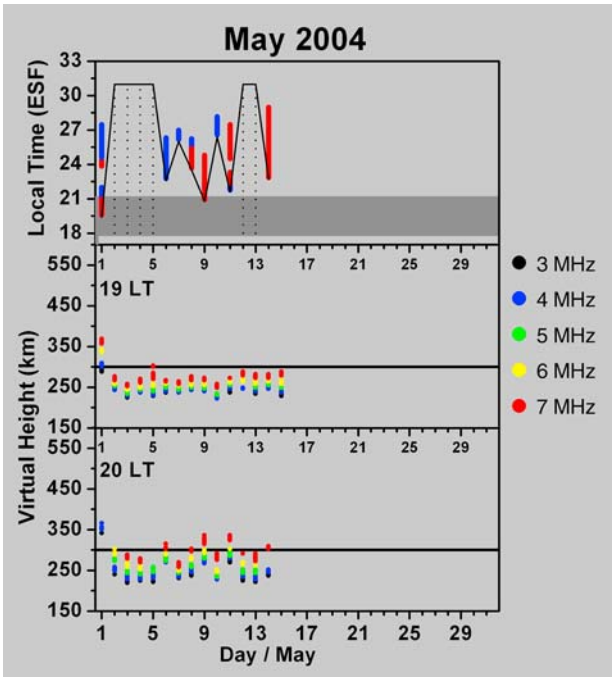

Figure 5. (continued)

Therefore, when the PRE causes the *F* layer bottom side to reach heights above 300 km there is a strong tendency for fresh ESF formation.

[27] 2. Since the electric field PRE is modulated by TPWID wave like oscillations, then the fresh ESF generation has some dependence on the TPWID phase.

[28] 3. The maximum TPWID phase, during the low ESF season, causes the electric field PRE to uplift the *F* layer bottom side above 300 km, thus creating favorable conditions for fresh ESF generation.

[29] 4. During the high ESF season, the electric field PRE usually causes the *F* layer bottom side to reach heights above 350 km, but, in some occasions, the TPWIDs at the minimum phase push the *F* layer downward to heights below 300 km. In these occasions there is suppression of fresh ESF formation.

[30] 5. The TPWIDs phase modulates the onset time of fresh ESF generation during high fresh ESF season. The modulation acts in such a way that, when the TPWID phase maximizes, the fresh ESF onset time occurs earlier, and, when the TPWID phase minimizes, the onset time occurs later.

[31] 6. The modulation of the electric field PRE amplitude by the TPWIDs is affected by short time perturbations related to geomagnetic storms. Therefore, if the *F* layer moves up (above 300 km) due to geomagnetic storms, then favorable conditions are created for fresh ESF generation. On the other hand, if the geomagnetic storms push down the *F* layer, then unfavorable conditions are created for fresh ESF generation.

[32] **Acknowledgments.** Thanks are due to the Brazilian funding agencies FAPESP and CNPq for the partial financial support through grants FAPESP 08/05482–5 and CNPq 301222/2003–7.

[33] Amitava Bhattacharjee thanks M. Keskinen and another reviewer for their assistance in evaluating this paper.

References

Abalde, J. R., P. R. Fagundes, J. A. Bittencourt, and Y. Sahai (2001), Observations of equatorial *F* region plasma bubbles using simultaneous OI 777.4 nm and OI 630.0 nm imaging: New results, *J. Geophys. Res.*, *106*(A12), 30,331–30,336, doi:10.1029/2001JA001115.

Abalde, J. R., P. R. Fagundes, Y. Sahai, V. G. Pillat, A. A. Pimenta, and J. A. Bittencourt (2004), Height-resolved ionospheric drifts at low latitudes from simultaneous OI 777.4 nm and OI 630.0 nm imaging observations, *J. Geophys. Res.*, *109*, A11308, doi:10.1029/2004JA010560.

Abalde, J. R., Y. Sahai, P. R. Fagundes, F. Becker-Guedes, J. A. Bittencourt, V. G. Pillat, W. L. C. Lima, C. M. N. Candido, and T. F. de Freitas (2009), Day-to-day variability in the development of plasma bubbles associated with geomagnetic disturbances, *J. Geophys. Res.*, *114*, A04304, doi:10.1029/2008JA013788.

Abdu, M. A. (2001), Outstanding problems in the equatorial ionosphere-thermosphere electrodynamics relevant to spread *F*, *J. Atmos. Sol. Terr. Phys.*, *63*, 869–884, doi:10.1016/S1364-6826(00)00201-7.

Abdu, M. A., I. Batista, and J. Sobral (1992), A new aspect of magnetic-declination control of equatorial spread *F* and *F* region dynamo, *J. Geophys. Res.*, *97*(A10), 14,897–14,904, doi:10.1029/92JA00826.

Abdu, M. A., K. N. Iyer, R. T. de Medeiros, I. S. Batista, and J. H. A. Sobral (2006a), Thermospheric meridional wind control of equatorial spread *F* and evening prereversal electric field, *Geophys. Res. Lett.*, *33*, L07106, doi:10.1029/2005GL024835.

Abdu, M. A., P. P. Batista, I. S. Batista, C. G. M. Brum, A. J. Carrasco, and B. W. Reinisch (2006b), Planetary wave oscillations in mesospheric winds, equatorial evening prereversal electric field and spread, *Geophys. Res. Lett.*, *33*, L07107, doi:10.1029/2005GL024837.

Abdu, M. A., T. K. Ramkumar, I. S. Batista, C. G. M. Brum, H. Takahashi, B. W. Reinisch, and J. H. A. Sobral (2006c), Planetary wave signatures in the equatorial atmosphere-ionosphere system, and mesosphere-*E*-and *F*-region coupling, *J. Atmos. Sol. Terr. Phys.*, *68*, 509–522, doi:10.1016/j.jastp.2005.03.019.

Bittencourt, J. A., Y. Sahai, P. R. Fagundes, and H. Takahashi (1997), Simultaneous observations of equatorial *F* region plasma depletions and thermospheric winds, *J. Atmos. Sol. Terr. Phys.*, *59*, 1049–1059, doi:10.1016/S1364-6826(96)00071-5.

Booker, H. G., and H. W. Wells (1938), Scattering of radio waves by the *F* region of the opnosphere, *Terr. Magn. Atmos. Electr.*, *43*(3), 249–256, doi:10.1029/TE043i003p00249.

Devasia, C. V., N. Jyoti, K. S. V. Subbarao, K. S. Viswanathan, D. Tiwari, and R. Sridharan (2002), On the plausible linkage of thermospheric meridional winds with the equatorial spread *F*, *J. Atmos. Sol. Terr. Phys.*, *64*, 1–12, doi:10.1016/S1364-6826(01)00089-X.

Fagundes, P. R., I. Y. Saha, J. A. Bittencourt, and H. Takahashi (1995), Relationship between generation of equatorial *F*-region plasma bubbles and thermospheric dynamics, *Adv. Space Res.*, *16*(5), 117–120, doi:10.1016/0273-1177(95)00180-M.

Fagundes, P. R., Y. Sahai, I. S. Batista, M. A. Abdu, J. A. Bittencourt, and H. Takahashi (1999), Observations of day-to-day variability in precursor signatures to equatorial *F* region plasma depletions, *Ann. Geophys.*, *17*, 1053–1063, doi:10.1007/s00585-999-1053-x.

Fagundes, P. R., V. G. Pillat, M. J. A. Bolzan, Y. Sahai, F. Becker-Guedes, J. R. Abalde, S. L. Aranha, and J. A. Bittencourt (2005), Observations of *F* layer electron density profiles modulated by planetary wave type oscillations in the equatorial ionospheric anomaly region, *J. Geophys. Res.*, *110*, A12302, doi:10.1029/2005JA011115.

Fagundes, P. R., V. Klausner, Y. Sahai, V. G. Pillat, F. Becker-Guedes, F. C. P. Bertoni, M. J. A. Bolzan, and J. R. Abalde (2007), Observations of daytime F2-layer stratification under the southern crest of the equatorial ionization anomaly region, *J. Geophys. Res.*, *112*, A04302, doi:10.1029/2006JA011888.

Fagundes, P. R., J. A. Bittencourt, J. R. Abalde, Y. Sahai, M. J. A. Bolzan, and W. L. C. Lima (2009), *F* layer postsunset height rise due to electric field prereversal enhancement: 1. Traveling planetary wave ionospheric disturbance effects, *J. Geophys. Res.*, doi:10.1029/2009JA014390, in press.

Fritts, D. C., et al. (2008), Gravity wave and tidal influences on equatorial spread *F* based on observations during the spread *F* experiment (SpreadFEx), *Ann. Geophys.*, *26*, 3235–3252.

Jyoti, N., C. V. Devasia, R. Sridharan, and D. Tiwari (2004), Threshold height (h′F)(c) for the meridional wind to play a deterministic role in the bottom side equatorial spread *F* and its dependence on solar activity, *Geophys. Res. Lett.*, *31*, L12809, doi:10.1029/2004GL019455.

Kil, H., R. DeMajistre, and L. J. Paxton (2004), *F* region plasma distribution seen from TIMED/GUVI and its relation to the equatorial spread *F* activity, *Geophys. Res. Lett.*, *31*, L05810, doi:10.1029/2003GL018703.

Klausner, V., P. R. Fagundes, Y. Sahai, C. M. Wrasse, V. G. Pillat, and F. Becker-Guedes (2009), Observations of GW/TID oscillations in the *F*2 layer at low latitude during high and low solar activity, geomagnetic quiet

and disturbed periods, *J. Geophys. Res.*, *114*, A02313, doi:10.1029/2008JA013448.
Lastovicka, J., P. Krizan, P. Sauli, and D. Novatna (2003), Persistence of the planetary wave type oscillations in foF2 over Europe, *Ann. Geophys.*, *21*, 1543–1552.
Lee, C. C., J. Y. Liu, B. W. Reinisch, W. S. Chen, and F. D. Chu (2005), The effects of the pre-reversal drift, the EIA asymmetry, and magnetic activity on the equatorial spread *F* during solar maximum, *Ann. Geophys.*, *23*, 745–751.
Mendillo, M., J. Meriwether, and M. Biondi (2001), Testing the thermospheric neutral wind suppression mechanism for day-to-day variability of equatorial spread *F*, *J. Geophys. Res.*, *106*(A3), 3655–3663, doi:10.1029/2000JA000148.
Mendillo, M., J. Baumgardner, X. Pi, P. J. Sultan, and R. Tsunoda (1992), Onset conditions for equatorial spread *F*, *J. Geophys. Res.*, *97*(A9), 13,865–13,876, doi:10.1029/92JA00647.
Mendillo, M., E. Zesta, S. Shodhan, P. J. Sultan, R. Doe, Y. Sahai, and J. Baumgardner (2005), Observations and modeling of the coupled latitude-altitude patterns of equatorial plasma depletions, *J. Geophys. Res.*, *110*, A09303, doi:10.1029/2005JA011157.
Nicolls, M. J., and M. C. Kelley (2005), Strong evidence for gravity wave seeding of an ionospheric plasma instability, *Geophys. Res. Lett.*, *32*, L05108, doi:10.1029/2004GL020737.
Ossakow, S. L. (1981), Spread *F* theories: A review, *J. Atmos. Terr. Phys.*, *43*(5–6), 437–452, doi:10.1016/0021-9169(81)90107-0.
Pancheva, D. V., et al. (2006), Two-day wave coupling of the low-latitude atmosphere-ionosphere system, *J. Geophys. Res.*, *111*, A07313, doi:10.1029/2005JA011562.
Pimenta, A. A., P. R. Fagundes, J. A. Bittencourt, and Y. Sahai (2001a), Relevant aspects of equatorial plasma bubbles under different solar activity conditions, *Adv. Space Res.*, *27*(6-7), 1213–1218, doi:10.1016/S0273-1177(01)00200-9.
Pimenta, A. A., P. R. Fagundes, J. A. Bittencourt, Y. Sahai, D. Gobbi, A. F. Medeiros, M. J. Taylor, and H. Takahashi (2001b), Ionospheric plasma bubble zonal drift: A methodology using OI 630 nm all-sky imaging systems, *Adv. Space Res.*, *27*(6-7), 1219–1224, doi:10.1016/S0273-1177(01)00201-0.
Pimenta, A. A., P. R. Fagundes, Y. Sahai, J. A. Bittencourt, and J. R. Abalde (2003), Equatorial *F* region plasma depletion drifts: Latitudinal and seasonal variations, *Ann. Geophys.*, *21*, 2315–2322.
Rao, P. V. S. R., P. T. Jayachandran, and P. S. Ram (1997), Ionospheric irregularities: The role of the equatorial ionization anomaly, *Radio Sci.*, *32*(4), 1551–1557.
Sahai, Y., P. R. Fagundes, and J. A. Bittencourt (2000), Transequatorial *F* region ionospheric plasma bubbles: Solar cycle effects, *J. Atmos. Sol. Terr. Phys.*, *62*, 1377–1383, doi:10.1016/S1364-6826(00)00179-6.
Saito, S., and T. Maruyama (2006), Ionospheric height variations observed by ionosondes along magnetic meridian and plasma bubble onsets, *Ann. Geophys.*, *24*, 2991–2996.
Sastri, J. H., M. A. Abdu, I. S. Batista, and J. H. A. Sobral (1997), Onset conditions of equatorial (range) spread *F* at Fortaleza, Brazil, during the June solstice, *J. Geophys. Res.*, *102*(A11), 24,013–24,021, doi:10.1029/97JA02166.
Sekar, R., R. Suhasini, and R. Raghavarao (1995), Evolution of plasma bubbles in the equatorial *F* region with different seeding conditions, *Geophys. Res. Lett.*, *22*(8), 885–888, doi:10.1029/95GL00813.
Sobral, J. H. A., M. A. Abdu, H. Takahashi, M. J. Taylor, E. R. de Paula, C. J. Zamlutti, M. G. de Aquino, and G. L. Borba (2002), Ionospheric plasma bubble climatology over Brazil based on 22 years (1977–1998) of 630 nm airglow observations, *J. Atmos. Sol. Terr. Phys.*, *64*, 1517–1524, doi:10.1016/S1364-6826(02)00089-5.
Sreeja, V., C. Vineeth, T. K. Pant, S. Ravindran, and R. Sridharan (2009), Role of gravity wavelike seed perturbations on the triggering of ESF: A case study from unique dayglow observations, *Ann. Geophys.*, *27*, 313–318.
Sultan, P. J. (1996), Linear theory and modeling of the Rayleigh-Taylor instability leading to the occurrence of equatorial spread *F*, *J. Geophys. Res.*, *101*(A12), 26,875–26,891, doi:10.1029/96JA00682.
Takahashi, H., L. M. Lima, C. M. Wrasse, M. A. Abdu, I. S. Batista, D. Gobbi, R. A. Buriti, and P. P. Batista (2005), Evidence on 2–4 day oscillations of the equatorial ionosphere h′F and mesospheric airglow emissions, *Geophys. Res. Lett.*, *32*, L12102, doi:10.1029/2004GL022318.
Takahashi, H., C. M. Wrasse, D. Pancheva, M. A. Abdu, I. S. Batista, L. M. Lima, P. P. Batista, B. R. Clemesha, and K. Shiokawa (2006), Signatures of 3–6 day planetary waves in the equatorial mesosphere and ionosphere, *Ann. Geophys.*, *24*, 3343–3350.
Takahashi, H., et al. (2007), Russell signatures of ultra fast Kelvin waves in the equatorial middle atmosphere and ionosphere, *Geophys. Res. Lett.*, *34*, L11108, doi:10.1029/2007GL029612.
Terra, P. M., J. H. A. Sobral, M. A. Abdu, J. R. Souza, and H. Takahashi (2004), Plasma bubble zonal velocity variations with solar activity in the Brazilian region, *Ann. Geophys.*, *22*, 3123–3128.
Tsunoda, R. T. (2005), On the enigma of day-to-day variability in equatorial spread *F*, *Geophys. Res. Lett.*, *32*, L08103, doi:10.1029/2005GL022512.
Tsunoda, R. T. (2009), Multi-reflected echoes: Another ionogram signature of large-scale wave structure, *Geophys. Res. Lett.*, *36*, L01102, doi:10.1029/2008GL036221.
Vineeth, C., T. K. Pant, C. V. Devasia, and R. Sridharan (2007), Atmosphere-ionosphere coupling observed over the dip equatorial MLTI region through the quasi 16-day wave, *Geophys. Res. Lett.*, *34*, L12102, doi:10.1029/2007GL030010.
Woodman, R. F. (2009), Spread *F*: An old equatorial aeronomy problem finally resolved, *Ann. Geophys.*, *27*, 1915–1934.

J. R. Abalde, P. R. Fagundes, G. Francisco, V. G. Pillat, and Y. Sahai, Laboratório de Física e Astronomia, Universidade do Vale do Paraíba, Sao Jose dos Campos, Sao Paulo, Brazil.
A. Bittencourt, Divisão de Aeronomia, Instituto Nacional de Pesquisas Espaciais, Sao Jose dos Campos, Sao Paulo, Brazil.
W. L. C. Lima, Observatório de Física Espacial, Centro Universitário Luterano de Palmas, Palmas, TO, Brazil.